archives
of thermodynamics
Vol. **35**(2014), No. 3, 251–264

On numerical modelling of heat transfer and fluid flow in a scraped surface heat exchanger

PRZEMYSŁAW BŁASIAK[1]
ZBIGNIEW GNUTEK

Wroclaw University of Technology, Wybrzeże Wyspiańskiego 27,
50-370 Wrocław, Poland

Abstract Steady state two-dimensional numerical simulation of laminar heat transfer and fluid flow in a scraped surface heat exchanger (SSHE) is presented. Typical SSHE consists of a stator, rotating shaft and scraping blades. Due to symmetry only a quarter of the heat exchanger is modelled. Governing equations for transport of mass, momentum and energy are discretised and solved with the use of commercial CFD code. The results are presented in a nondimensional form for velocity, pressure and temperature distributions. Local and averaged Nusselt number along the stator wall are calculated and depicted in graphs. It was found that the thirty fold increase of the cReynolds number, leads to heat transfer enhancement rate by three times.

Keywords: Scraped surface heat exchanger; Nusselt number; Thermal boundary layer

Nomenclature

A	–	surface area, m^2
c_p	–	specific heat, $\mathrm{J/(kg\,K)}$
d	–	shaft diameter, m
D	–	stator diameter, m
g	–	gravitational acceleration, $\mathrm{m/s}^2$
Gr	–	Grashof number, $\mathrm{Gr} = \frac{\rho^2 g \beta \Delta T \left(\frac{D-d}{2}\right)^3}{\eta^2}$
h	–	enthalpy, J/kg
k	–	thermal conductivity, $\mathrm{W/(m\,K)}$

[1]Corresponding Author. E-mail: przemyslaw.blasiak@pwr.edu.pl

n	–	rotational speed, rev/s
Nu	–	Nusselt number, $\mathrm{Nu} = -\left(\frac{D-d}{2}\right)\frac{\partial\Theta}{\partial r}$
Pr	–	Prandtl number, $\mathrm{Pr} = \frac{c_p\eta}{k}$
p	–	pressure, Pa
P	–	nondimensional pressure
r	–	radius, m
$\mathbf{r}$	–	position vector, m
Re	–	mixing Reynolds number, $\mathrm{Re} = \frac{\omega D^2\rho}{2\pi n}$
T	–	temperature, K
v_r, v_γ	–	radial and tangential components of the absolute velocity, m/s
v	–	absolute velocity
V_r, V_γ	–	non-dimensional components of the absolute velocity
q''	–	heat flux, $\mathrm{W/m^2}$

Greek symbols

β	–	thermal expansion coefficient, 1/K
Γ	–	length of the arc, m
ΔT	–	temperature difference, K
η	–	dynamic viscosity, Pa s
γ	–	angle, rad
Θ	–	dimensionless temperature
ν	–	kinematic viscosity, $\mathrm{m^2/s}$
ρ	–	density, $\mathrm{kg/m^3}$
ω	–	angular velocity, rad/s

Subscripts

T	–	parameters at the top wall (stator)
B	–	parameters at the bottom wall (shaft)
rel	–	relative rotating frame of reference

1 Introduction

Scraped surface heat exchangers (SSHE) are widely used in chemical and food industries for thermal treatment of the working fluid, crystallization and various continuous processes [1, 2]. They are especially dedicated to high viscosity fluids, i.e., characterized by large values of Prandtl number Pr. Standard SSHE unit is presented in Fig. 1. It consists of three main parts: cylindrical pipe (stator) of diameter D, rotating shaft (rotor) of diameter d and blades (scrapers). However there are many types of SSHE. Another configuration of the blades is shown in Fig. 2, where the scrapers are attached to the wall via springs. This configuration is chosen for the analysis purposes in the present paper.

The working fluid is pumped through an annular gap formed by the cylindrical pipe and the shaft. On the outer surface of the stator wall, heat-

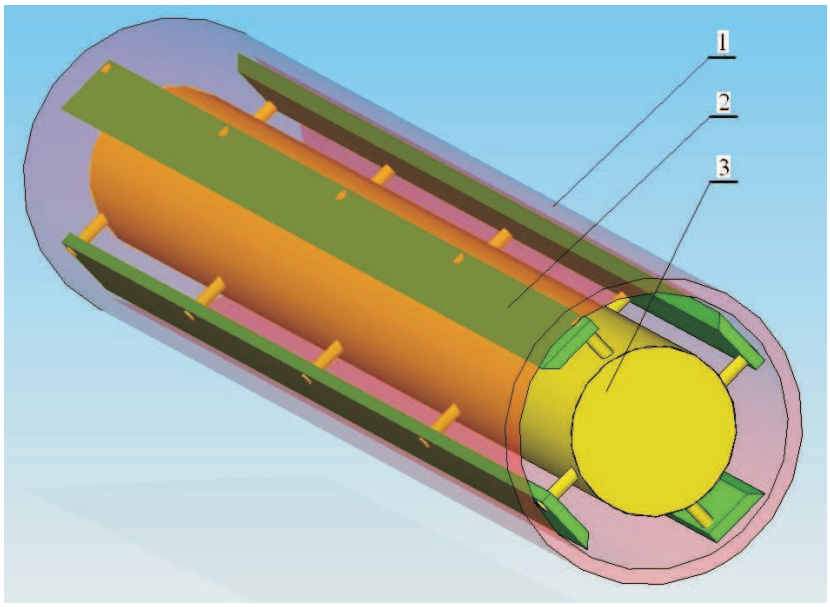

Figure 1: Standard construction of the scraped surface heat exchanger: 1) stator, 2) blade, 3) rotor.

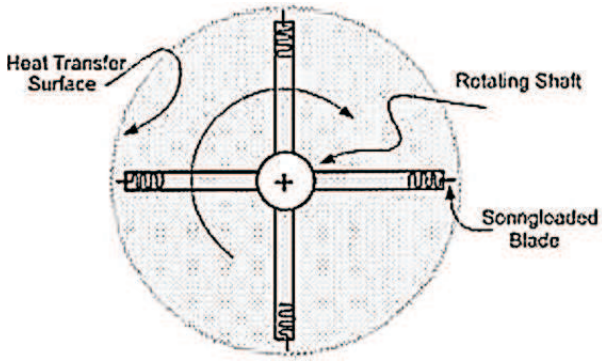

Figure 2: Cross-section of the scraped surface heat exchanger [3].

ing or cooling jacket is usually used in order to provide appropriate conditions for the thermal treatment process. The scrapers are used to enhance heat transfer rate from working fluid to the stator wall. Augmentation in heat transfer rate is caused by combination of two mechanisms. The first is the so-called scraping of the thermal boundary layer phenomenon. During

the fluid flow with simultaneous heat transfer, near the wall a thin region is formed, where the highest temperature gradient prevails. This layer constitutes the main part of thermal resistance in a heat exchange process. The blades move in the close vicinity of the stator wall and continuously scrape off the fluid from it. Consequently the thermal resistance is mechanically removed and heat flux through the wall increases. The second mechanism is a mixing of the bulk fluid with fluid elements localized near the wall. The mixing effect is caused both by rotating movement of the blades and by centrifugal forces emerging from rotation of the whole mass of the working fluid induced by the blades.

Heat transfer and fluid flow in the SSHE is a very complex phenomenon. Fully three-dimensional analysis of this problem is a difficult task and a high computational power is required. All works encountered in the literature are concerned with fluids featuring high Prandtl number and there is a lack of the data for fluids exhibiting low Prandtl number. In the presented study a simple two-dimensional numerical model of the SSHE is given in order to get ithe nsight into the thermal-hydraulic phenomena occurring in such devices. The working fluid was air with $\mathrm{Pr} = 0.71$, which is regarded as a low value of Prandtl number. The main goal was to investigate the influence of flow conditions on the rate of heat transfer. Parameter varied during the simulations is the Reynolds number Re, which represents the importance of inertial forces relative to the viscosity forces. Heat transfer rate is expressed by the nondimensional heat transfer coefficient, i.e., the Nusselt number.

2 Mathematical model

Two-dimensional steady state fluid flow and heat transfer are modelled in the scraped surface heat exchanger for the geometry configuration presented in Fig. 2. Due to the symmetry only a quarter of the heat exchanger cross-section is modelled. Resulting numerical domain and the boundary conditions are depicted in Fig. 3. The cylinder diameter and the shaft diameter are denoted by D and d, respectively. The working fluid, treated as Newtonian and incompressible, is heated via a constant heat flux, q'', imposed on the shaft surface. On the cylinder surface, the cold temperature, T_T, is applied. The blades move in the clockwise direction and are assumed to be infinitesimally thin and adiabatic. The flow is considered as laminar and fluid properties (density, ρ, specific heat capacity, c_p, thermal conductiv-

ity, k, thermal expansion coefficient, β, dynamic viscosity, η) are constant. Viscous dissipation and gravitational forces are also neglected. On each of the walls, the so-called no-slip boundary condition is applied and walls are treated as impermeable.

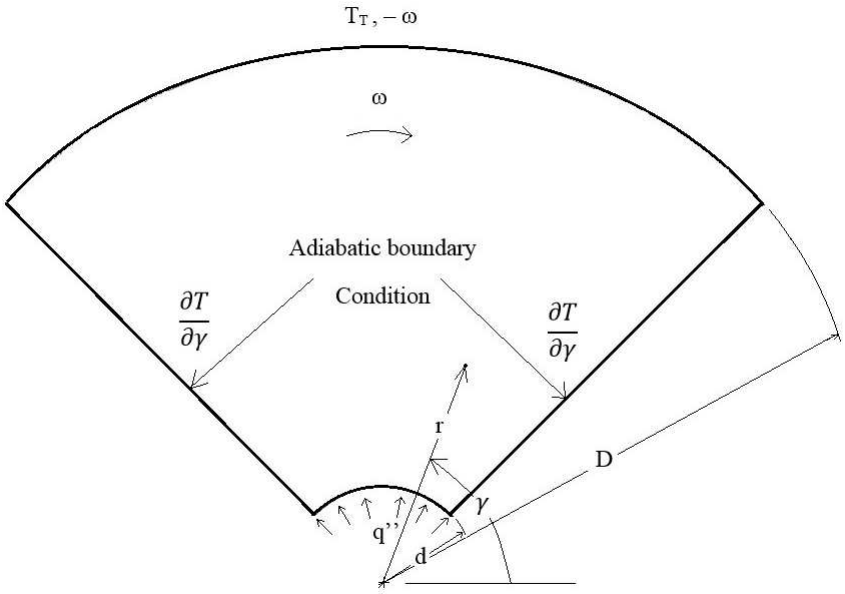

Figure 3: Numerical domain and boundary conditions.

The governing equations for the present problem are transport equation of mass, momentum and energy. They are solved in the rotating frame [4,5] and can be written in the following vector form:

$$\nabla \cdot \mathbf{v}_{rel} = 0\,, \tag{1}$$

$$\nabla\cdot(\mathbf{v}_{rel}\mathbf{v}_{rel})+2\boldsymbol{\omega}\times\mathbf{v}_{rel}+\boldsymbol{\omega}\times\boldsymbol{\omega}\times\mathbf{r} = -\frac{\nabla p}{\rho}+\nu\nabla\cdot\left[\left(\nabla\mathbf{v}_{rel}+\nabla\mathbf{v}_{rel}^{T}\right)-\frac{2}{3}\nabla\mathbf{v}_{rel}\mathbf{I}\right]\,, \tag{2}$$

$$\nabla\cdot(\rho\mathbf{v}_{rel}H_{rel}) = \nabla\cdot(k\nabla T)\ , \tag{3}$$

where $\mathbf{I}$ is the unit matrix, superscript T denotes transposition, and $\mathbf{v}_{rel}$ is a relative velocity defined as follows

$$\mathbf{v}_{rel} = \mathbf{v} - \boldsymbol{\omega}\times\mathbf{r}\ , \tag{4}$$

where $\mathbf{v}$ is the absolute velocity, $\boldsymbol{\omega}$ is the given angular velocity, and $\mathbf{r}$ is the position vector. In the energy equation, Eq. (3), H_{rel} is the relative total enthalpy defined in the following form:

$$H_{rel} = h + \frac{1}{2}\left(v_{rel}^2 - |\boldsymbol{\omega} \times \mathbf{r}|^2\right) \ . \tag{5}$$

Applied boundary conditions have the following form:

$$\left.\begin{array}{llllll} r = D/2, & \frac{\pi}{4} < \theta < \frac{3}{4}\pi, & v_r = 0, & v_\gamma = -\omega D/2, & T = T_T, \\ r = d/2, & \frac{\pi}{4} < \theta < \frac{3}{4}\pi, & v_r = 0, & v_\gamma = \omega d/2, & \frac{\partial T}{\partial r} = -q''/k, \\ \gamma = \frac{\pi}{4}, & d/2 < r < D/2, & v_r = 0, & v_\gamma = \omega r/2, & \frac{\partial T}{\partial \gamma} = 0, \\ \gamma = \frac{3}{4}\pi, & d/2 < r < D/2, & v_r = 0, & v_\gamma = \omega r/2 & \frac{\partial T}{\partial \gamma} = 0, \end{array}\right\} , \tag{6}$$

where v_r and v_γ are radial and tangential components of the absolute velocity respectively.

The governing parameters of the problem are: mixing Reynolds number Re [6] (with adopted $n = \omega/(2\pi)$), Grashof, Gr, and Prandtl, Pr, which are found to be:

$$\mathrm{Re} = \frac{\omega D^2 \rho}{2\pi\eta} \ , \quad \mathrm{Gr} = \frac{\rho^2 g \beta \Delta T \left(\frac{D-d}{2}\right)^3}{\eta^2} \ , \quad \mathrm{Pr} = \frac{c_p \eta}{k} \ , \tag{7}$$

where temperature difference, ΔT, is

$$\Delta T = \frac{q''\left(\frac{D-d}{2}\right)}{k} \ . \tag{8}$$

In order to analyse heat transfer rate, the local Nusselt number, Nu, and the area-averaged Nusselt number, $\overline{\mathrm{Nu}}$, are calculated. These are defined as

$$\mathrm{Nu} = -\left(\frac{D-d}{2}\right)\left.\frac{\partial \Theta}{\partial r}\right|_{r=D/2} , \quad \overline{\mathrm{Nu}} = \frac{1}{\Gamma}\int_0^\Gamma \mathrm{Nu}\, d\Gamma \ , \tag{9}$$

where Γ is the length of the arc and Θ is the nondimensional temperature constructed as follows:

$$\Theta = \frac{T - T_T}{\overline{T}_B - T_T} \ , \tag{10}$$

where T_T is the temperature at the stator wall, and $\overline{T}_B$ is an area-averaged temperature at the shaft surface A_B and is calculated from the following formula:

$$\overline{T}_B = \frac{\int_{A_B} T_B dA}{A_B} \,. \tag{11}$$

Velocity and pressure are nondimensionalised as follows:

$$V_r = \frac{2v_r}{\omega\, D}, \quad V_\gamma = \frac{2v_\gamma}{\omega\, D}, \quad P = \frac{2p}{\rho\,(\omega\, D)^2} \tag{12}$$

3 Results and discussion

Four numerical simulations were carried out. The governing equations were discretized and solved with the use of commercial CFD (computational fluid dynamics) software [7]. The resolution of the numerical mesh was 1024 x 1024 and consisted of hexahedral elements. Mesh nodes were uniformly distributed. Reynolds number was in the range $100 \leqslant \mathrm{Re} \leqslant 3162$, while Pr and Gr were kept constant and were equal to 0.71 and 10^4, respectively. Range of Reynolds number results from the series of Richardson number, $\mathrm{Ri} = \mathrm{Gr}/\mathrm{Re}^2$, which was taken as 1.0, 0.1, 0.01, and 0.001. Richardson number represents the magnitude of natural convection relative to the forced convection. It is a commonly used parameter to designating the convection flow regime.

Calculations were stopped if the following conditions were met [8]:

$$\frac{\left|\Psi^{n+1}(i,j) - \Psi^{n}(i,j)\right|}{\mathrm{Max}\left|\Psi^{n+1}(i,j)\right|} < 10^{-6} \quad \text{and} \quad \left|1.0 - \frac{\overline{\mathrm{Nu}}_T}{\overline{\mathrm{Nu}}_B}\right| < 10^{-2} \tag{13}$$

where i and j denote the coordinates of the nodes on the numerical mesh, n is the iteration loop counter, Ψ is a dependent variable (v_r, v_γ or T). The numbers $\overline{\mathrm{Nu}}_T$ and $\overline{\mathrm{Nu}}_B$ are area-averaged Nusselt numbers on the top and bottom wall respectively. In the steady state, condition $\overline{\mathrm{Nu}}_B = \overline{\mathrm{Nu}}_T$ should be satisfied, due to heat flux on the bottom wall must be the same as on the top wall. Calculations were carried out for a fixed geometrical configuration in which $d/D = 0.17857$.

Plots of streamlines in terms of normalized velocity are presented in Fig. 4. For low Re streamlines are curved and smooth. With the increasing Re streamlines are flattened in the center of the numerical domain and near the shaft. The highest velocities occur near the tip of the blades as could be expected. In every case the lowest velocities occur in two areas. The first region is located near the shaft, where the lowest values of tangential

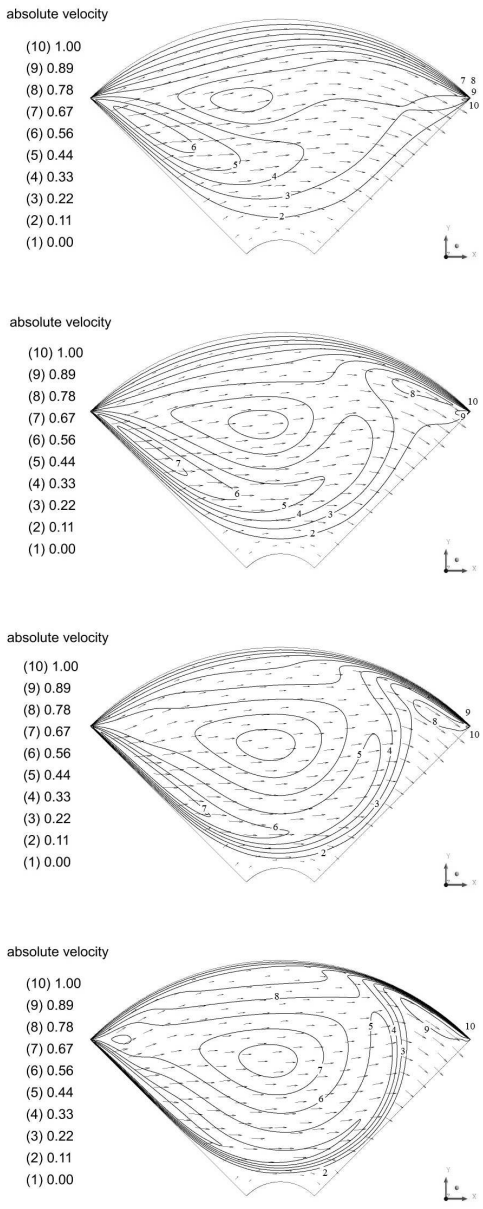

Figure 4: Distribution of streamlines in terms of nondimensional velocity for four different Reynolds numbers. From top to bottom Re = 100, 316, 1000, and 3162, respectively.

component of the velocity prevail. The second area is localized near the stator wall, except of the near-blade region. It is surprising that fluid flows with higher velocities in the central part of the exchanger and not near the stator wall. In the region adjoined to heat exchange wall, low velocities exist, compared to central and near-blade areas of the heat exchanger. It results in diminishing of the heat transfer efficiency. With increasing Re, the centrifugal forces increase and the zone in the right top corner of the numerical domain, where the highest velocities prevail, develops. One can expect the highest rate of heat transfer in this area.

In Fig. 5 distributions of the nondimensional pressure P for four different Reynolds numbers are shown. For the low Re, pressure distribution is uniform. Only in the right and the left top corners extreme values exist. Local minimum and maximum of the pressure occur in the right and left top corner respectively. With an increase of Re the zones in the right and left top corners develop. The highest pressure prevails in the top region of the numerical domain, due to increasing influence of centrifugal forces. An increase of centrifugal forces causes that pressure in the near-shaft region decreases.

In Fig. 6 distributions of isotherms of the non-dimensional temperature Θ are depicted for four different Reynolds numbers. The predicted temperature fields are essentially established by the movement of the blades and centrifugal forces. For the lowest value of Re a large area with the highest temperature gradients is localized near the right blade. With an increasing Re, this region shrinks and flattens into the shaft direction. Fluid moved by the blades and centrifugal forces transports thermal energy mainly via convection mechanism. The increase of Re diminishes diffusion effects on heat transfer. Additionally, the nondimensional temperature increases, what indicates that heat transfer is augmented. It is caused by stronger circulation of the fluid moved by the blades and increase of the centrifugal forces. For $\mathrm{Re} = 3162$ almost the whole numerical domain has a uniform temperature distribution.

It is evident that temperature gradients are located near the downstream (right) scraper. It is triggered out by the mechanism of scraping of the thermal boundary layer. Just behind the blade this layer is very thin, what results in a low thermal resistance and high heat flux. It is confirmed in Fig. 7, where the distributions of the local Nu along the cylinder wall are presented. With the increase of Re the rate heat transfer increases and it is expressed by the increase of Nu. For the lowest value of Re, curve rises

mildly and the maximum is about ≈ 5. However with the increase of Re, curve is very steep in the region near the blade and Nu tends to infinity as the thickness of the thermal boundary layer tends to zero. For further parts of the cylinder wall Nu distinctly decreases, what is caused by rebuilding of the thermal boundary layer and low values of velocity. Thin region, where the highest Nu occur, implies that rebuilding of the thermal boundary layer is very fast. Moreover, one can see that for the maximal value of Re flow is strongly disturbed by the blades and curve for Nu distribution has now two maxima, as opposed to other cases, where it monotonically decreases to zero.

In the Tab. 1 the values of area-averaged $\overline{\mathrm{Nu}}$ over shaft (bottom) and cylinder (top) surfaces are summarized. For each case the condition for $\overline{\mathrm{Nu}}$ from Eq. (13) were met. The highest error did not exceed 0.3%.

Table 1: Average Nusselt numbers $\overline{\mathrm{Nu}}$ on the top and the bottom wall.

Pr	Re	$\overline{\mathrm{Nu}}$		$\left\lvert 1-\frac{\overline{\mathrm{Nu}}_T}{\overline{\mathrm{Nu}}_B}\right\rvert$
		Top	Bottom	%
0.71	100	5.34	5.34	0.02
	316	8.06	8.05	0.05
	1000	11.54	11.55	0.06
	3162	15.86	15.90	0.26

4 Conclusion

Numerical simulations of heat transfer and fluid flow in a two-dimensional SSHE were reported. The transport equations were written and solved in noninertial cylindrical system of coordinates. In simulation results a strong influence of Reynolds number on the heat transfer rate has been revealed. With an increase of this parameter the local and mean Nusselt number increase. The highest values of Nusselt numbers occur just behind the downstream blade in the right top corner. It is due to scraping of the thermal boundary layer phenomenon and mixing effect induced by centrifugal forces. Thermal boundary layer is the thinnest in this region, what results in the low thermal resistance. Scraping effect of the blades manifests in augmentation of heat transfer rate. Thirty fold increase of Reynolds number,

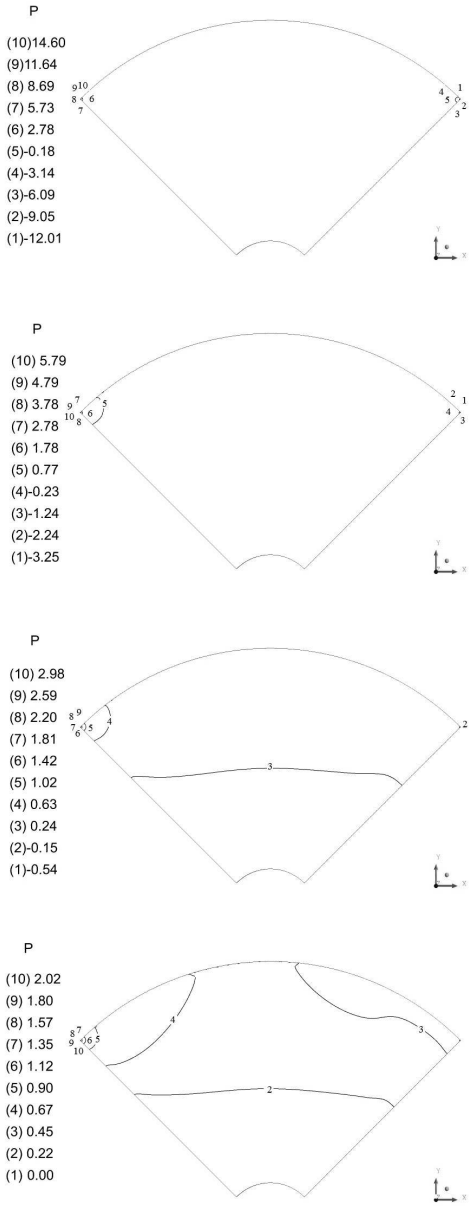

Figure 5: Distribution of nondimensional pressure P for four different Reynolds numbers. From top to bottom Re = 100, 316, 1000 , and 3162, respectively.

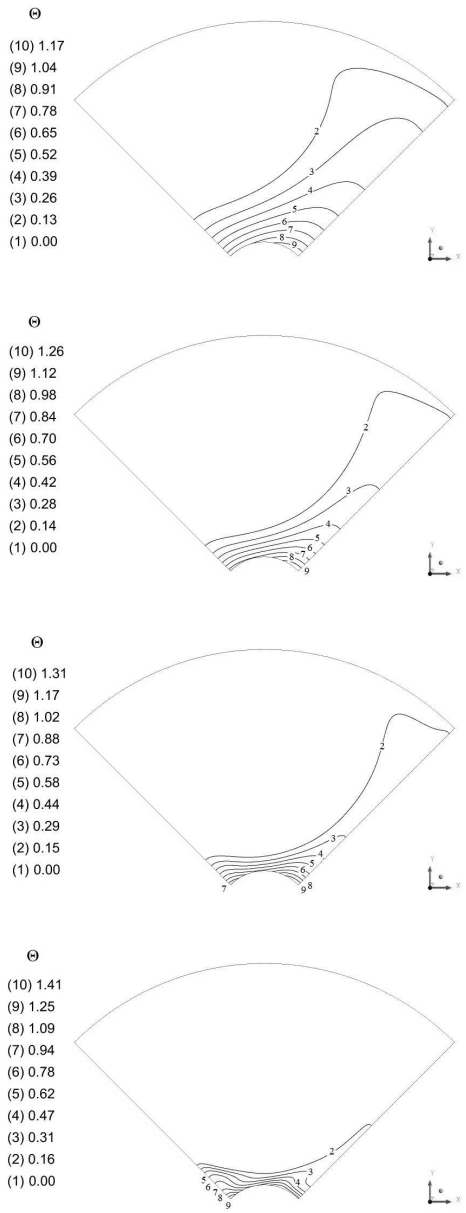

Figure 6: Distribution of isotherms of nondimensional temperature Θ for four different Reynolds numbers. From top to bottom Re = 100, 316, 1000, and 3162, respectively.

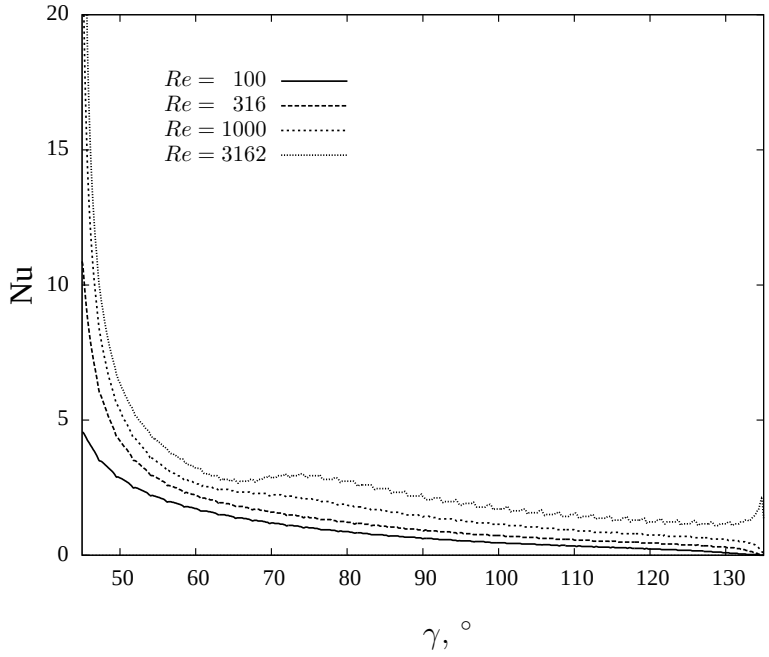

Figure 7: Distribution of local Nusselt number along the cylinder wall for four different Reynolds numbers.

enhances the heat transfer rate three times. Augmentation does not make an impression, however for fluids with higher Prandtl number, the scraping effect should be much more pronounced. Nevertheless present results can be helpful in heat transfer analysis in scroll compressors [9] due to thermal boundary layer scraping phenomenon naturally occuring in such machines.

Acknowledgements Calculations have been carried out using resources provided by Wroclaw Centre for Networking and Supercomputing (http://wcss.pl).

Received 18 June 2014

References

[1] Patience D.B., Rawlings J.B., Mohameed A.H.: *Crystalization of para-xylene in scraped surface crystalizers.* AICHE J. **47**(2001), 2441–2451.

[2] Rao C.S., Hartel R.W.: *Scraped surface heat exchangers*. Crit. Rev. Food Sci. Nutr. **46**(2006), 207–219.

[3] Hewitt G.F., Shires G.L., Bott T.R.: *Process heat transfer*. Begell House, London 1994.

[4] Paul E.L., Atiemo-Obeng V.A., Kresta S.M.: *Industrial mixing. Science and practice*. Wiley, New Jersey 2004.

[5] Schobeiri M.: *Turbomachinery Flow Physics and Dynamic Performance*. Springer, Berlin 2005.

[6] Stręk F.: *Mixing and mixers*, WNT, Warsaw 1971 (in Polish).

[7] ANSYS Academic Research, User Guide 14.5, ANSYS, Inc.

[8] Moallemi M.K., Jang K.S.: *Prandtl number effects on laminar mixed concection heat transfer in a lid-driven cavity*. Int. J. Heat Mass Tran. **35**(1992), 8, 1881–1892.

[9] Rak J.: *The thermal-flow behavior of the working chamber in an oil-free scroll compressor*. Arch. Thermodyn. **34**(2013), 3, 161–172.